Addressing the Deconvolution Problem in DVCS/DVMP Through String-Based GPDs

Kiminad Mamo (William & Mary)

May 19, 2025 @ QCD Evolution, Jefferson Lab, Newport News, VA

References

This talk is based on:

- **2411.04162** (PRL) (with Ismail Zahed)
- **2404.13245** (PRD) (with Ismail Zahed)
- **2206.03813** (PRD) (with Ismail Zahed)

AdS/CFT

- The AdS/CFT correspondence can be used to compute correlation functions of local operators [Maldacena (1998); Gubser, Klebanov, Polyakov (1998); Witten (1998)]:

$$Z_{\text{gauge}}(J\mathcal{O}, N_c, \lambda) \;\equiv\; Z_{\text{gravity}}(\phi_0, g_5, \alpha'/R^2), \quad \text{where } J \equiv \phi_0.$$

- Correlation functions are evaluated via Witten diagrams in AdS.
- For non-conformal theories with a mass gap (dual to a deformed AdS background), scattering amplitudes can likewise be computed using these Witten diagrams in AdS

$$ds^2 = \frac{R^2}{z^2}\left(\eta_{\mu\nu}\, dx^\mu dx^\nu - dz^2\right), \quad \eta_{\mu\nu} = \mathrm{diag}(1, -1, -1, -1),$$

with $0 \leq z \leq \infty$, connects the UV boundary ($z \to 0$) to the IR ($z \to \infty$), and mass gap/confinement induced by a background dilaton field $\phi(z) = \kappa^2 z^2$.

Spin-2/0 (Gravitational) Form Factors of Proton

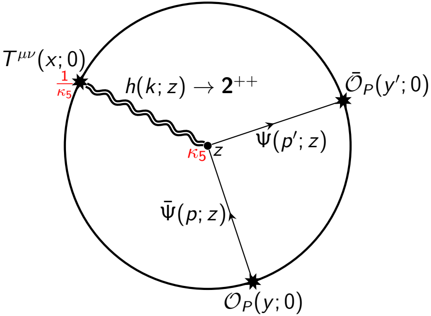

Figure: Witten diagram for spin-2 gravitational form factor due to the exchange 2^{++} glueballs with $\kappa_5^2 \sim \frac{1}{N_c^2}$.

$$A(K,\kappa_T) \;=\; \frac{1}{2}\int dz\,\sqrt{g}\,e^{-\phi}\,z\,\left(\psi_R^2(z)+\psi_L^2(z)\right)\sum_{n=0}^{\infty}\frac{\sqrt{2}\,\kappa_5\,F_n\,\psi_n(z)}{K^2+m_n^2}.$$

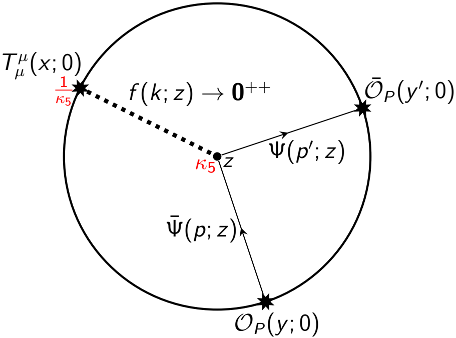

Figure: Witten diagram for scalar gravitational form factor due to the exchange 0^{++} glueballs.

$$D(K,\kappa_T,\kappa_S) = -\frac{4\,m_N^2}{3\,K^2}\Big[A(K,\kappa_T)\ -\ A_S(K,\kappa_S)\Big],$$

Comparison with Lattice Data

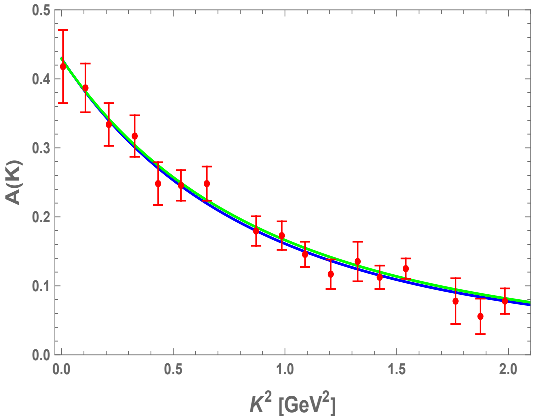

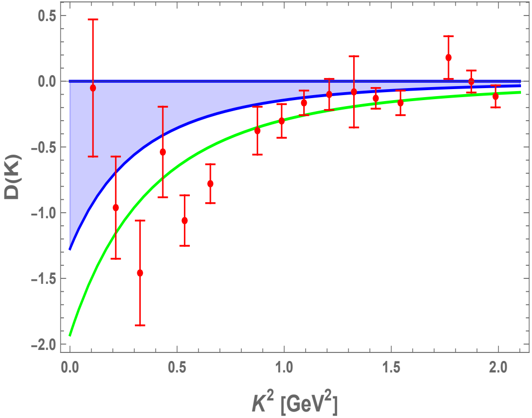

Recent lattice QCD results [Pefkou:2021] (red points) compared to holographic fits (blue curves) with $\kappa_T = 0.388\,\mathrm{GeV}$, $\kappa_S = 0.217\,\mathrm{GeV}$. The green line is a tripole fit to the same lattice data.

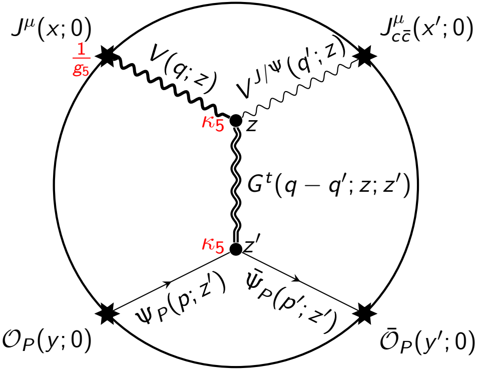

Figure: Witten diagrams for the holographic photo/electroproduction of J/Ψ with $g_5^2 \sim \frac{1}{N_c}$ and $\kappa_5^2 \sim \frac{1}{N_c^2}$.

Photoproduction of heavy mesons near threshold

- the differential cross section for photoproduction of heavy vector mesons (J/ψ or Υ), near threshold, is given by

$$\frac{d\sigma}{dt} = \mathcal{N}^2 \times \left[A(t) + \eta^2 D(t)\right]^2 \times \frac{1}{A^2(0)} \times \frac{1}{32\pi(s-m_N^2)^2} \times F(s,t,M_V,m_N) \times \left(1 - \frac{t}{4m_N^2}\right)$$

with the normalization factor $\mathcal{N}$ defined as

$$\mathcal{N}^2 \equiv e^2 \times \left(\frac{f_V}{M_V}\right)^2 \times \mathbb{V}^2_{h\gamma^* J/\Psi} \times (2\kappa_5^2)^2 \times A^2(0) = 7.768^2\,\mathrm{nb/GeV^6}$$

- note that $F(s,t) \sim s^4 \sim 1/\eta^4$ with the amplitude $\mathcal{A} \sim s^2 \times A(t) + s^0 \times D(t)$ as expected from 2^{++} and 0^{++} glueball t-channel exchanges

Extraction of the 2^{++} glueball contribution

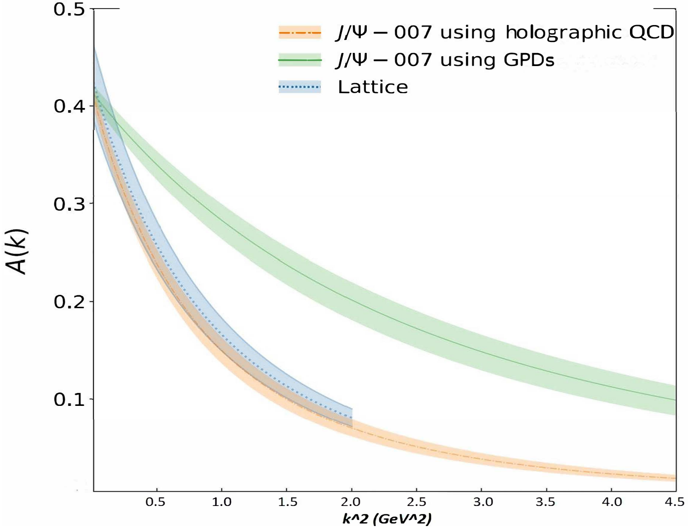

Extraction of the 0^{++} glueball contribution

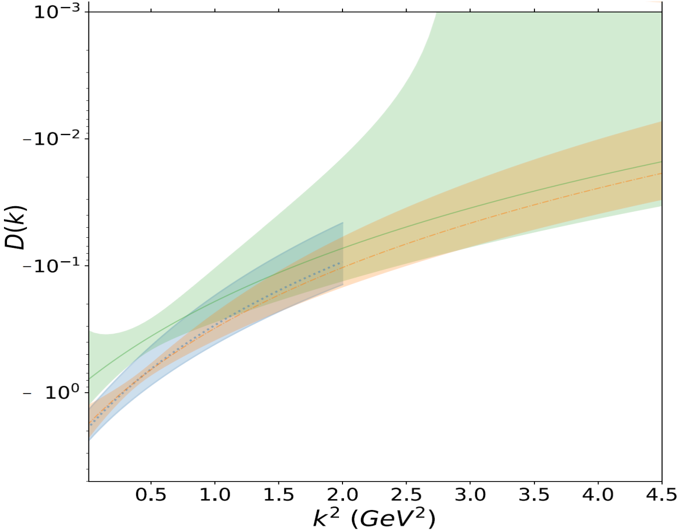

Electroproduction of heavy mesons near threshold

- the differential cross section for electroproduction of heavy vector mesons (J/ψ or Υ), near threshold, is given by

$$\frac{d\sigma(s,t,Q,M_{J/\Psi},\epsilon_T,\epsilon'_T)}{dt} \propto \mathcal{I}^2(Q,M_{J/\Psi}) \times \left(\frac{s}{\kappa^2}\right)^2 \times \left[A(t)+\eta^2 D(t)\right]^2$$

$$\frac{d\sigma(s,t,Q,M_{J/\Psi},\epsilon_L,\epsilon'_L)}{dt} \propto \frac{1}{9} \times \frac{Q^2}{M^2_{J/\Psi}} \times \mathcal{I}^2(Q,M_{J/\Psi}) \times \left(\frac{s}{\kappa^2}\right)^2 \times \left[A(t)+\eta^2 D(t)\right]^2$$

- where we defined the transition form factor that controls the Q dependence as

$$\mathcal{I}(Q, M_{J/\Psi}) = \frac{\mathcal{I}(0, M_{J/\Psi})}{\frac{1}{6} \times \left(\frac{Q^2}{4\kappa_{J/\Psi}^2} + 3\right)\left(\frac{Q^2}{4\kappa_{J/\Psi}^2} + 2\right)\left(\frac{Q^2}{4\kappa_{J/\Psi}^2} + 1\right)},$$

with $\mathcal{I}(0, M_{J/\Psi}) = \frac{g_5 f_{J/\Psi}}{4M_{J/\Psi}}$

Spin-j Form Factor of Proton

- the spin-j form factors of proton can be defined as

$$
\begin{aligned}
\langle p_2 | T^{\mu_1\mu_2\ldots\mu_j}(0) | p_1\rangle = \overline{u}(p_2)\Bigg(&\mathcal{A}(k,j)\gamma^{\mu_1}p^{\mu_2}\ldots p^{\mu_j} + \mathcal{B}(k,j)\frac{ip^{\mu_1}p^{\mu_3}\ldots p^{\mu_j}\sigma^{\mu_2\alpha}k_\alpha}{2m_N} \\
&+ \mathcal{C}(k,j)\frac{k^{\mu_1}k^{\mu_2}\ldots k^{\mu_j} - \eta^{\mu_1\mu_2}\eta^{\mu_3\mu_4}\ldots\eta^{\mu_{j-1}\mu_j}k^2}{m_N}\Bigg)u(p_1)
\end{aligned}
$$

Spin-j Form Factor of Proton

- the spin-j form factor, can be computed using the Witten diagram

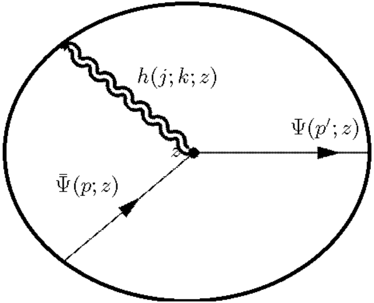

Figure: Witten diagram for the spin-j form factor due to the exchange of spin-j glueball resonances.

Four-point correlation functions $<\bar{P}J_\mu J_\nu P>$ with spin-j exchange

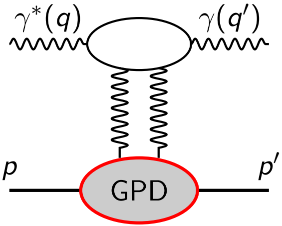

collinear factorization

$\equiv$

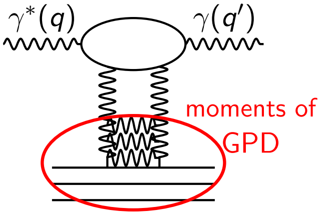

with BFKL kernel

$\equiv$

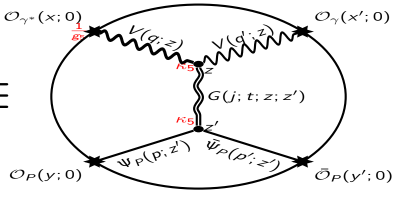

with BPST (holographic) kernel

- the scattering amplitude using the BFKL kernel:

$$\mathrm{Im}\,\mathcal{A}_{\gamma^*_{L/T}p\to Vp}(j,s,t) = \int_0^\infty k_\perp\,\mathrm{d}k_\perp \int_{k_\perp}^\infty k'_\perp\,\mathrm{d}k'\;\Phi_A(k_\perp,Q)\,G(j;t;k_\perp;k'_\perp)\,\Phi_B(k'_\perp)\,,$$

$$\mathrm{Im}\,\mathcal{A}_{\gamma^*_{L/T}p\to Vp}(s,t) = \int_{C-i\infty}^{C+i\infty}\frac{\mathrm{d}j}{2\pi i}\left(\frac{s}{s_0}\right)^{j-1} I(j,Q)\times F(j,t)$$

Four-point correlation functions $< \bar{P} J_\mu J_\nu P >$ with spin-j exchange

Feature	BFKL ($\lambda \ll 1$)	BPST ($\lambda \gg 1$)
Transverse variable	$k_\perp$	$z \propto k_\perp$
Differential kernel	$k_\perp^2 \partial_{k_\perp}^2 + k_\perp \partial_{k_\perp} - \frac{4}{D_p}(j - j_0^p)$	$k_\perp^2 \partial_{k_\perp}^2 + k_\perp \partial_{k_\perp} - \frac{4}{D_h}(j - j_0^h)$
Intercept shift	$j_0^p = 1 + \frac{\lambda \ln 2}{\pi^2}$	$j_0^h = 2 - \frac{2}{\sqrt{\lambda}}$
Diffusion width	$D_p = \frac{7\,\zeta(3)}{2\pi^2}\lambda$	$D_h = \frac{2}{\sqrt{\lambda}}$

Four-point correlation functions $<\bar{P} J_\mu J_\nu P>$ with spin-j exchange

- the scattering amplitude using the holographic kernel:

$$\begin{aligned}
\mathcal{A}_{\gamma^*_{L/T} p \to V p}(j,s,t) \quad &\sim \quad -\frac{1}{g_5} \times 2\kappa^2 \times \mathcal{V}_{h\gamma^*_{L/T} V}(j,Q) \times \mathcal{V}_{h\bar{\Psi}\Psi}(j,t) \\
&\times \quad \left[q^{\mu_1} q^{\mu_2} ... q^{\mu_j} \, P_{\mu_1\mu_2...\mu_j;\nu_1\nu_2...\nu_j}(k) \, p_1^{\nu_1} p_1^{\nu_2} ... p_1^{\nu_j}\right] \\
&\times \quad \frac{1}{m_N} \times \bar{u}(p_2) u(p_1)
\end{aligned}$$

Four-point correlation functions $< \bar{P} J_\mu J_\nu P >$ with spin-j exchange

- we use the identity

$$q^{\mu_1} q^{\mu_2} ... q^{\mu_j} \, P_{\mu_1 \mu_2 ... \mu_j ; \nu_1 \nu_2 ... \nu_j}(m_n, k) \, p_1^{\nu_1} p_1^{\nu_2} ... p_1^{\nu_j} = (p_1 \cdot q)^j \times \hat{d}_j(\eta, t)$$

with

$$\hat{d}_j(\eta, t) = {}_2F_1 \left(-\frac{j}{2}, \frac{1-j}{2}; \frac{1}{2} - j; \frac{4m_N^2}{-t} \times \eta^2 \right)$$

where the skewness parameter is given by $\eta \sim \frac{k \cdot q}{2 p_1 \cdot q}$. Also note that, for $j = 2$, we have the massive spin-2 projection operator $P_{\mu_1 \mu_2 ; \nu_1 \nu_2}(k) \equiv P_{\mu\nu;\alpha\beta}(k)$ defined as

$$P_{\mu\nu;\alpha\beta}(k) = \frac{1}{2} \left(P_{\mu;\alpha} P_{\nu;\beta} + P_{\mu;\beta} P_{\nu;\alpha} - \frac{2}{3} P_{\mu;\nu} P_{\alpha;\beta} \right)$$

which is written in terms of the massive spin-1 projection operator

$$P_{\mu;\alpha}(k) = \eta_{\mu\alpha} - k_\mu k_\alpha / k^2$$

Four-point correlation functions $< \bar{P} J_\mu J_\nu P >$ with spin-j exchange

- separating the skewness η dependent and independent part, we can rewrite the scattering amplitude as

$$
\begin{aligned}
\mathcal{A}_{\gamma^*_{L/T} p \to V p}(j,s,t) \;\; &\sim \;\; -\frac{1}{g_5} \times 2\kappa^2 \times \mathcal{V}_{h\gamma^*_{L/T} V}(j,Q) \times [\mathcal{A}(j,t) + \mathcal{D}_\eta(j,\eta,t)] \\
&\times \;\; (p_1 \cdot q)^j \times \frac{1}{m_N} \times \bar{u}(p_2) u(p_1)
\end{aligned}
$$

where

$$
\mathcal{D}_\eta(j,\eta,t) \;\; = \;\; \left(\hat{d}_j(\eta,t) - 1\right) \times [\mathcal{A}(j,t) - \mathcal{A}_S(j,t)]
$$

with

$$
\mathcal{A}_S(j,t) \;\; \equiv \;\; \mathcal{A}(j, ; \kappa_T \to \kappa_S)
$$

Holographic parametrization of conformal moments of gluon GPDs

- our holographic parametrization of conformal moments of gluon GPD at finite skewness, and at input scale $\mu = \mu_0$, is given by

$$\mathbb{F}_g^{(+)}(j, \eta, t; \mu_0) = \mathcal{A}_g(j, t; \mu_0) + \mathcal{D}_{g\eta}(j, \eta, t; \mu_0)$$

  for even $j = 2, 4, \ldots$
- we use

$$\mathcal{A}_g(j, t; \mu_0) = \int_0^1 dx \, x^{j-2} \, xg(x; \mu_0) \, x^{a_T}$$

  with the input gluon PDF $xg(x; \mu_0)$ at $\mu = \mu_0$, and $a_T \equiv -\alpha'_T t$

Holographic parametrization of conformal moments of gluon GPDs

- the skewness or η-dependent terms are fixed by holography as

$$\mathcal{D}_{g\eta}(j,\eta,t;\mu_0) = \left(\hat{d}_j(\eta,t) - 1\right) \times \left[\mathcal{A}_g(j,t;\mu_0) - \mathcal{A}_{gS}(j,t;\mu_0)\right]$$

where

$$\mathcal{A}_{gS}(j,t;\mu_0) \;\equiv\; \mathcal{A}_g(j,t;\mu_0,\alpha'_T \to \alpha'_S)$$

- the A-form factor of the gluon gravitational form factor of the proton is given by

$$A_g(t;\mu_0) = \mathcal{A}_g(j=2,t;\mu_0)$$

and the D-form factor (or the D-term) of the gluon gravitational form factor of the proton is

$$\eta^2 D_g(t;\mu_0) = \mathcal{D}_{g\eta}(j=2,\eta,t;\mu_0)$$

Holographic parametrization of conformal moments of non-singlet quark GPDs

- the holographic parametrization of the conformal moments of the non-singlet (valence) quark GPDs at $\mu = \mu_0$ is given by

$$\mathbb{F}_q^{(-)}(j, \eta, t; \mu_0) = \mathcal{F}_q^{(-)}(j, t; \mu_0) + \mathcal{F}_{q\eta}^{(-)}(j, \eta, t; \mu_0)$$

for odd $j = 1, 3, \cdots$, where we have defined

$$\mathcal{F}_q^{(-)}(j, t; \mu_0) = \int_0^1 dx\, x^{j-1}\, q_v(x; \mu_0)\, x^{a_q}$$

with the input valence (non-singlet) quark PDF $q_v(x; \mu_0) = q(x; \mu_0) - \bar{q}(x; \mu_0) = H_q^{(-)}(x, \eta = 0, t = 0; \mu_0)$ at $\mu = \mu_0$, and $a_q \equiv -\alpha'_q t$, where α'_q is a Regge slope parameter

Holographic parametrization of conformal moments of non-singlet quark GPDs

- we also have the flavor combinations

$$\mathbb{F}^{(-)}_{u\pm d}(j,\eta,t;\mu_0) = \int_0^1 dx\, \frac{u_v(x;\mu_0) \pm d_v(x;\mu_0)}{x^{1-j+\alpha'_{u\pm d}t}}$$

  assuming $\bar{u}(x,\mu_0) = \bar{d}(x,\mu_0)$
- we fix $\alpha'_{u\pm d}$, using the experimental Dirac electromagnetic form factor of the proton ($F_{1p}(t)$) and neutron ($F_{1n}(t)$) from their valence combination

$$\mathbb{F}^{(-)}_{u+d}(1,\eta,t;\mu_0) = 3\left(F_{1p}(t) + F_{1n}(t)\right)\,,$$

  and the isovector combination

$$\mathbb{F}^{(-)}_{u-d}(1,\eta,t;\mu_0) = F_{1p}(t) - F_{1n}(t)$$

Holographic parametrization of conformal moments of singlet quark GPDs

- the holographic parametrization of the conformal moments of the singlet (sea) quark GPDs at $\mu = \mu_0$ are given by

$$\sum_{q=1}^{N_f} \mathbb{F}_q^{(+)}(j, \eta, t; \mu_0) = \sum_{q=1}^{N_f} \mathcal{F}_q^{(+)}(j, t; \mu_0) + \mathcal{F}_{q\eta}^{(+)}(j, \eta, t; \mu_0)$$

for even $j = 2, 4, \cdots$, where we have defined

$$\sum_{q=1}^{N_f} \mathcal{F}_q^{(+)}(j, t; \mu_0) = \int_0^1 dx\, x^{j-1} \sum_{q=1}^{N_f} q^{(+)}(x; \mu_0)\, x^{a_q}$$

with the input singlet quark PDF $\sum_{q=1}^{N_f} q^{(+)}(x; \mu_0) = \sum_{q=1}^{N_f} q(x; \mu_0) + \bar{q}(x; \mu_0) = \sum_{q=1}^{N_f} H_q^{(+)}(x, \eta = 0, t = 0; \mu_0)$ at $\mu = \mu_0$, and $a_q \equiv -\alpha_q' t$.

Holographic parametrization of conformal moments of singlet quark GPDs

- the skewness or η-dependent terms are given by

$$\sum_{q=1}^{N_f} \mathcal{F}_{q\eta}^{(+)}(j,\eta,t;\mu_0) = \left(\hat{d}_j(\eta,t) - 1\right) \times \left[\sum_{q=1}^{N_f} \mathcal{F}_{q}^{(+)}(j,t;\mu_0) - \mathcal{F}_{qS}^{(+)}(j,t;\mu_0)\right]$$

where

$$\sum_{q=1}^{N_f} \mathcal{F}_{qS}^{(+)}(j,t;\mu_0) \equiv \sum_{q=1}^{N_f} \mathcal{F}_{q}^{(+)}(j,t;\mu_0,\alpha'_q \to \alpha'_{qs})$$

Holographic parametrization of conformal moments of singlet quark GPDs

- the A-form factor of the quark gravitational form factor of proton is given by

$$\sum_{q=1}^{N_f} A_q(t;\mu_0) = \sum_{q=1}^{N_f} \mathcal{F}_q^{(+)}(j=2,t;\mu_0)$$

and the D-form factor (or the D-term) of the quark gravitational form factor of the proton is given by

$$\eta^2 \sum_{q=1}^{N_f} D_q(t;\mu_0) = \sum_{q=1}^{N_f} \mathcal{F}_{q\eta}^{(+)}(j=2,\eta,t;\mu_0)$$

Comparison of the conformal moments to lattice QCD

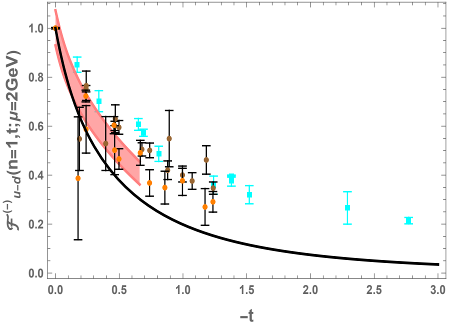

(a)

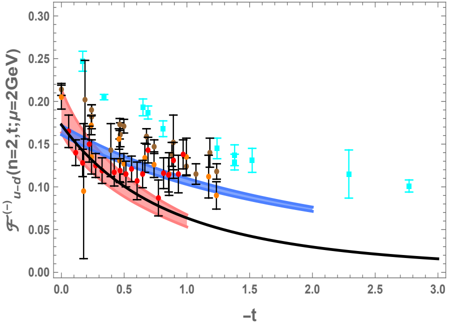

(b)

Figure: Our evolved moments of $u - d$ quark GPD $H^{u-d}(x, \eta, t; \mu)$ at $\mu = 2\ \mathrm{GeV}$ (black-solid line). The other colored curves and data points are lattice results from [Bhattacharya 2023] (Cyan data points), [LHPC 2007] (Orange and Brown data points), [Lin 2020] (Pink curve), [Alexandrou 2019] (Red data points), and [Hackett 2023] (Blue curve).

Comparison of the conformal moments to lattice QCD

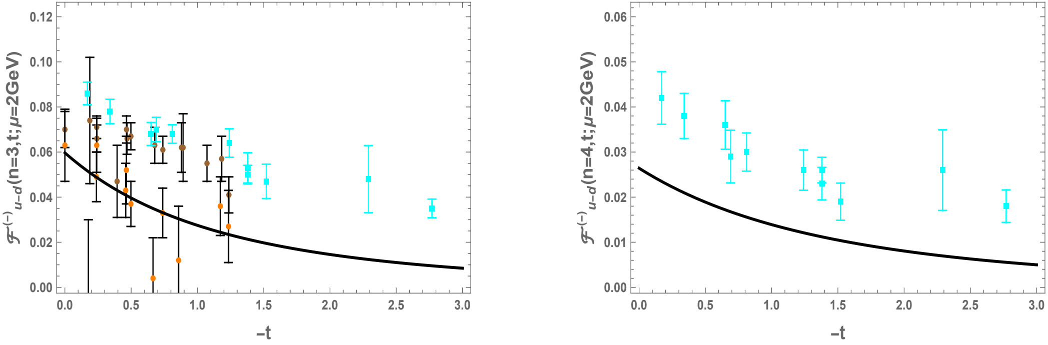

(a) (b)

Figure: Our evolved moments of $u-d$ quark GPD $H^{u-d}(x,\eta,t;\mu)$ at $\mu = 2\ \mathrm{GeV}$, are represented by black line. The other colored curves and data points, corresponding to lattice data, from various sources are shown for comparison.

Comparison of the conformal moments to lattice QCD

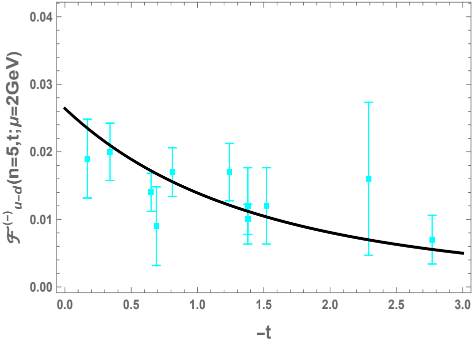

(a)

Figure: Our evolved moments of $u-d$ quark GPD $H^{u-d}(x,\eta,t;\mu)$ at $\mu = 2$ GeV, are represented by black line. The other colored curves and data points, corresponding to lattice data, from various sources are shown for comparison.

Comparison of the conformal moments to lattice QCD

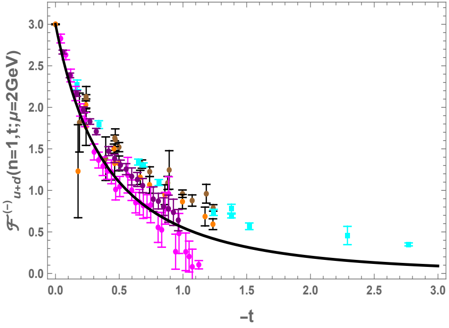

(a)

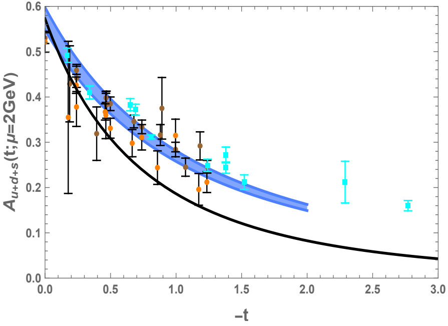

(b)

Figure: Our evolved moments of $u+d$ quark GPD $H^{u+d}(x,\eta,t;\mu)$ at $\mu = 2\ \mathrm{GeV}$ (black-solid line). The lattice results are from [Bhattacharya 2023] (Cyan data points), [LHPC 2007] (Orange and brown data points), [Alexandrou 2018] (Purple data points), [Djukanovic 2023] (Magenta data points), and [Hackett 2023] (Blue curve).

Comparison of the conformal moments to lattice QCD

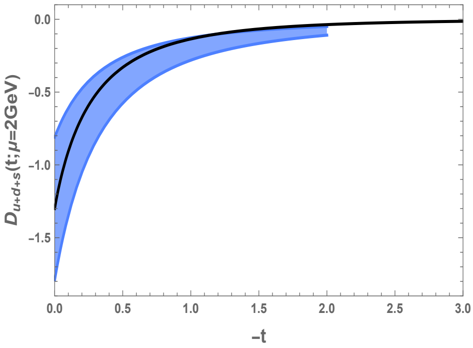

(a)

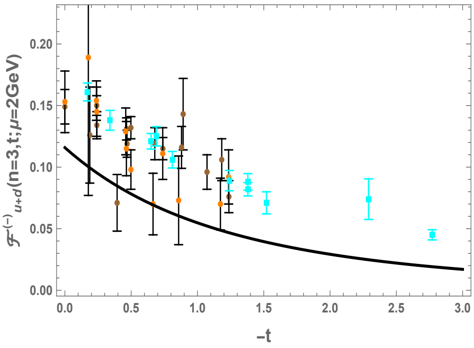

(b)

Figure: Our evolved moments of $u + d$ quark GPD $H^{u+d}(x, \eta, t; \mu)$ at $\mu = 2$ GeV, are represented by black line. The other colored curves and data points, corresponding to lattice data, from various sources are shown for comparison.

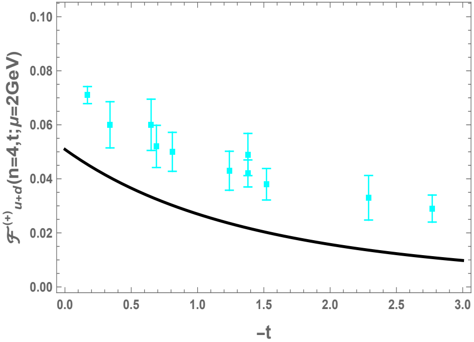

(a)

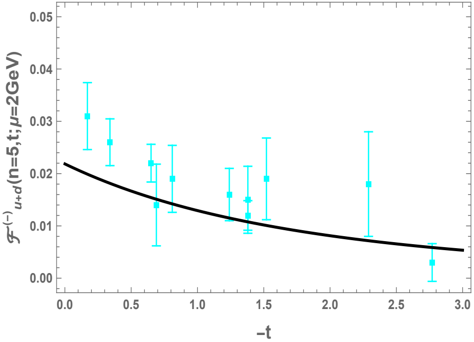

(b)

Figure: Our evolved moments of $u + d$ quark GPD $H^{u+d}(x, \eta, t; \mu)$ at $\mu = 2$ GeV, are represented by black line. The other colored curves and data points, corresponding to lattice data, from various sources are shown for comparison.

Comparison of the conformal moments to lattice QCD

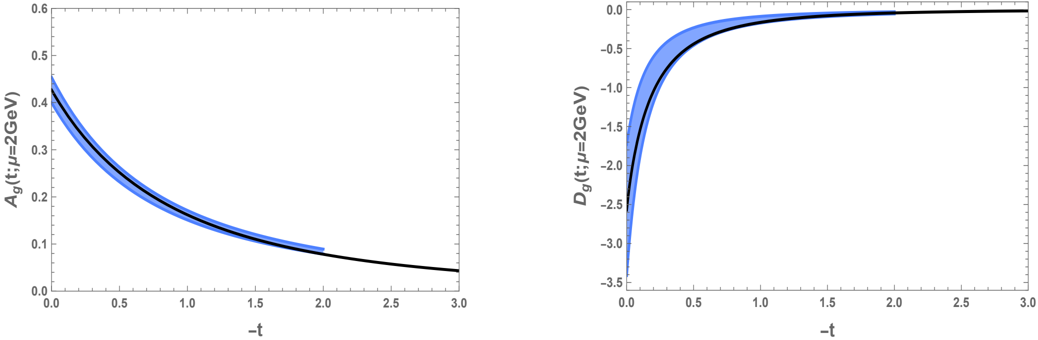

(a) (b)

Figure: Our evolved moments of gluon GPD $H_g^{(+)}(x, \eta, t; \mu)$ at $\mu = 2\ \mathrm{GeV}$, are represented by black line. The other colored curves and data points, corresponding to lattice data, from various sources are shown for comparison.

Reconstructing quark and gluon GPDs from their conformal moments

- the gluon GPD series expansion interms of their conformal (Gegenbauer) moments is extended to a Mellin-Barnes-type integral to facilitate the incorporation of complex-valued conformal spins [Mueller:2005]:

$$H_g^{(+)}(x,\eta,t;\mu) = \frac{1}{2i}\int_{\mathbb{C}} dj\, \frac{(-1)}{\sin(\pi j)} \left({}^g p_j(x,\eta) + {}^g p_j(-x,\eta)\right) \mathbb{F}_g^{(+)}(j,\eta,t;\mu),$$

with the partial waves

$${}^g p_j(x,\eta) = \theta(\eta - |x|)\frac{1}{\eta^{j-1}}{}^g\mathcal{P}_j\left(\frac{x}{\eta}\right) + \theta(x-\eta)\frac{1}{x^{j-1}}{}^g\mathcal{Q}_j\left(\frac{x}{\eta}\right)$$

$$\begin{aligned} {}^g\mathcal{P}_j\left(\frac{x}{\eta}\right) &= \left(1+\frac{x}{\eta}\right)^2 {}_2F_1\left(-j, j+1, 3\middle|\frac{1}{2}\left(1+\frac{x}{\eta}\right)\right)\frac{2^{j-1}\Gamma(3/2+j)}{\Gamma(1/2)\Gamma(j-1)} \\ {}^g\mathcal{Q}_j\left(\frac{x}{\eta}\right) &= {}_2F_1\left(\frac{j-1}{2}, \frac{j}{2}; \frac{3}{2}+j; \frac{\eta^2}{x^2}\right)\frac{\sin(\pi[j+1])}{\pi} \end{aligned}$$

Reconstructing quark and gluon GPDs from their conformal moments

- for quark GPDs we have

$$H_q^{(\pm)}(x,\eta,t;\mu) = \frac{1}{2i}\int_{\mathbb{C}} dj\, \frac{1}{\sin(\pi j)}\left(p_j(x,\eta) \mp p_j(-x,\eta)\right)\mathbb{F}_q^{(\pm)}(j,\eta,t;\mu),$$

with the partial waves

$$p_j(x,\eta) = \theta(\eta - |x|)\frac{1}{\eta^j}\mathcal{P}_j\left(\frac{x}{\eta}\right) + \theta(x-\eta)\frac{1}{x^j}\mathcal{Q}_j\left(\frac{x}{\eta}\right)$$

where

$$\begin{aligned}
\mathcal{P}_j\left(\frac{x}{\eta}\right) &= \left(1+\frac{x}{\eta}\right){}_2F_1\left(-j, j+1, 2\middle|\frac{1}{2}\left(1+\frac{x}{\eta}\right)\right) \times \frac{2^j\Gamma(3/2+j)}{\Gamma(1/2)\Gamma(j)} \\
\mathcal{Q}_j\left(\frac{x}{\eta}\right) &= {}_2F_1\left(\frac{j}{2}, \frac{j+1}{2}; \frac{3}{2}+j\middle|\frac{\eta^2}{x^2}\right) \times \frac{\sin(\pi j)}{\pi}
\end{aligned}$$

Reconstructing quark and gluon GPDs from their conformal moments

- The non-singlet isovector quark GPD, denoted as $H_{u-d}^{(-)}(x, \eta, t; \mu)$, represents the difference between the up and down quark distributions,

$$H_{u-d}^{(-)}(x, \eta, t; \mu) = \frac{1}{2i} \int_{\mathbb{C}} dj \, \frac{1}{\sin(\pi j)} \, p_j(x, \eta) \, \mathbb{F}_{u-d}^{(-)}(j, \eta, t; \mu)$$

- The analytically continued conformal PWs $p_j(x, \eta)$ have support $-\eta \leq x \leq 1$

Comparison of our reconstructed $u - d$ quark GPDs to lattice

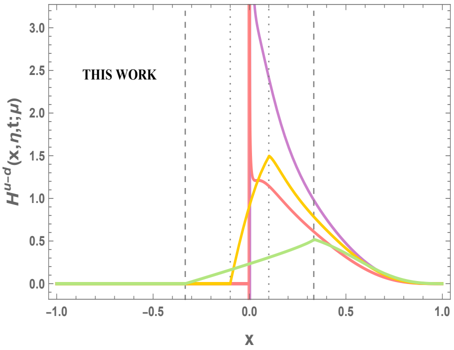

(a)

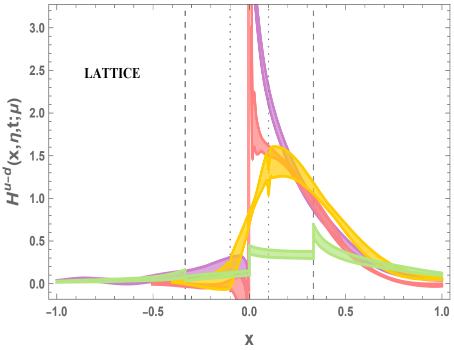

(b)

Figure: Purple for $\eta = 0$, $-t = 0$, green for $\eta = 1/3$, $-t = 0.69\ \mathrm{GeV}^2$, yellow for $\eta = 0.1$, $-t = 0.23\ \mathrm{GeV}^2$ (all with $\mu = 2\ \mathrm{GeV}$), and pink for $\eta = 0$, $-t = 0.39\ \mathrm{GeV}^2$, and $\mu = 3\ \mathrm{GeV}$. Lattice results: [Alexandrou 2020] (purple, and green curves), [Holligan,2023] (yellow curve), and [Lin 2020] (pink curve).

Thank You!